

1 Article

2 A methodologic approach for the selection of 3 bio-resorbable polymers in the development of 4 medical devices: the case of 5 poly(L-lactide-co- ϵ -caprolactone)

6 Alberto Cingolani ^{1,2}, Tommaso Casalini ^{1,3}, Stefano Caimi ¹, Antoine Klaue ¹, Mattia Sponchioni ⁴,
7 Filippo Rossi ^{4,*} and Giuseppe Perale ^{1,3,*}

8 ¹ Institute for Chemical and Bioengineering, Department of Chemistry and Applied Bioscience ETH
9 Zurich, Vladimir-Prelog-Weg 1-5/10, 8093 Zürich, Switzerland; A.C. alberto.cingolani@chem.ethz.ch; T.C.
10 tommaso.casalini@chem.ethz.ch; S.C. stefano.caimi@chem.ethz.ch; A.K. antoine.klaue@chem.ethz.ch.

11 ² Industrie Biomediche Insubri SA (IBI), Via Cantonale 67, 6805 Mezzovico-Vira, Switzerland

12 ³ Biomaterials Laboratory, Institute for Mechanical Engineering and Materials Technology, SUPSI –
13 University of Applied Sciences and Arts of Southern Switzerland. Via Cantonale 2C, Galleria 2, 6928
14 Manno, Switzerland; G.P. giuseppe.perale@supsi.ch;

15 ⁴ Department of Chemistry, Materials and Chemical Engineering “G. Natta”, Politecnico di Milano, 20100
16 Milan, Italy; M.S. mattia.sponchioni@polimi.it; F.R. filippo.rossi@polimi.it.

17 • Correspondence: filippo.rossi@polimi.it; Tel: +39 02-2399-3145
18 giuseppe.perale@supsi.ch; Tel.: +41-58-666-66-41
19

20

21 **Abstract:** In the last decades bioresorbable and biodegradable polymers have gained a very good
22 reputation both in research and in industry thanks to their unique characteristics. They are, indeed,
23 able to ensure high performances and biocompatibility, at the same time avoiding post-healing
24 surgical interventions for devices removal. In the medical device industrial use of such
25 biopolymers, it is widely known that product formulation and manufacturing need to follow
26 specific procedures in order to ensure both proper mechanical properties and desired degradation
27 profile. Moreover, also the sterilization method is crucial and its impact on physical properties is
28 generally underestimated. In this work we focused our attention on the effect of different terminal
29 sterilization methods on two commercially available poly(L-lactide-co- ϵ -caprolactone) with
30 equivalent chemical composition (70% PLA and 30% PCL) and relatively similar initial molecular
31 weight, but different chains arrangement and crystallinity. Results obtained show that crystallinity
32 plays a key role, helping in preserving the narrow distribution of chains and, as a consequence,
33 defined physical properties. These statements can be used as guidelines for a better choice of the
34 most adequate biodegradable polymers in the production of resorbable medical devices.

35 **Keywords:** electron beam; ethylene oxide; medical devices; polymers; sterilization.
36

37 1. Introduction

38 Biodegradable polymers have become, in the last decade, a major base material for the
39 development of many different bioresorbable medical devices[1–3]. Thanks to their intrinsic
40 characteristics and chemical and physical nature, they perfectly match with this kind of specific
41 application, as they ensure high performance, complete biocompatibility and tunable resorbability at
42 the same time[4–6].
43

44 Indeed, playing with initial composition of polymers and their molecular weights, mostly
45 derivatives of polylactic acid (PLA), of polyglycolic acid (PGA) and of polycaprolactone (PCL),
46 and/or their copolymers and blends, enables to perfectly combine desired mechanical characteristics,
47 with a fully bioresorbable product[7,8]. Specifically, they properly address the big disadvantage of
48 the post-healing surgical intervention for devices that needs to be implanted into the patient's
49 body[9], because, upon degradation, they will be naturally eliminated by the organism, without
50 necessity of direct removal[10–12].

51 These considerations, coupled with the intrinsic ease of processing and production of
52 polymer-based building blocks, both in the form of individual polymer chains[13] or in the micro
53 and nanoparticles fashion[14–16], make them a very robust path towards the development of
54 advanced medical devices and eventually also controlled drug delivery systems. Indeed, many
55 different applications have been properly exploited and developed, from biodegradable sutures
56 system[17], to polymer capsules for drug delivery application[14], hydrogels[18] for controlled drug
57 release and scaffold for cells in tissue engineering[19]. As mentioned before, the great advantage that
58 all of the aforementioned products have in common is that they will naturally disappear from the
59 patient's body in reasonable and controllable time after the implantation, leaving minimal traces and
60 small impact[1].

61 When dealing with implantable medical devices, it is very important to point out that, in the
62 industrial practice, product formulation and manufacturing need to follow specific procedures.
63 Indeed, once the desired inputs are defined (*i.e.* mechanical properties and degradation profile)
64 accurate selection of the base material needs to be done. This has to take into consideration not only
65 the characteristics of the pristine base polymer but also the way they will be affected by all the
66 manufacturing and post-processing steps.

67 As a matter of fact, processes such as thermoforming, injection molding, extrusion and in
68 general all of those that are performed at medium to high temperature and/or applying mechanical
69 stress can significantly alter the polymers features[20]. Moreover, though some steps might be
70 product dependent, certainly terminal sterilization represents in this sense not only a major point,
71 but also a crucial, necessary and compulsory passage in the production of every implantable medical
72 device[21,22]. Specifically, it aims at the inactivation of any microbiological contaminants that might
73 be present on the final products itself. Moreover, although preparation conditions might be perfectly
74 in accordance with quality management system guidelines (*i.e.* ISO 13485-2016), the finite outputs
75 can be considered sterile only if they are free from any viable microorganisms[23,24]. The necessity
76 on relying on a fully validated and fixed protocol, ensuring reliable and reproducible performances,
77 therefrom derives.

78 The most widely used industrial terminal sterilization techniques imply either steam, ethylene
79 oxide (EtO), γ or electron beam irradiation[25]. Regarding polymer-based devices, not all of the
80 aforementioned possibilities are available as, for example, steam and γ irradiation frequently cause
81 excessive degradation and changes in physical or mechanical properties, which can be detrimental
82 for intended performance, especially in terms of degradation rates and times and also device shapes
83 and dimensions[24,25]. Thus, the most conventional solutions in this sense, involve electron beam
84 radiations and exposition to alkylation agents (ethylene oxide)[23].

85 Apart from the composition and the molecular weights (M_w , M_n , PDI), that clearly have a role
86 in polymer response to all manufacturing and post-processing operations[20,26], and are generally
87 taken into consideration in product formulation, often also other crucial physical parameters (T_g , T_m ,
88 crystallinity)[27,28], might be of great interest, though many times neglected. A superficial
89 characterization generally leads to major issues when different raw materials suppliers or
90 formulations are required, especially because the final response to the whole production processing,
91 including sterilization, might not be identical[29].

92
93
94

95 In this work we decided to study the effect of the two most common different terminal
96 sterilization methods for resorbable biopolymers (EtO and electron beam) on two commercially
97 available poly(L-lactide-co- ϵ -caprolactone) with equivalent chemical composition (70% PLA and
98 30% PCL) and relatively similar initial molecular weight, but different chains arrangement and
99 crystallinity.

100 These polymers find application *e.g.* in the production of devices for hard tissues fixation and
101 regeneration[30–32]. As a matter of fact, it resulted that crystallinity, indeed, plays a role in the
102 response of these apparently equivalent polymers to different sterilization techniques, helping in
103 preserving the narrow distribution of chains and, as a consequence, defined physical properties.
104 Furthermore, we employed independent experimental data from literature in order to quantify the
105 impact of the sterilization on the actual degradation rate through mathematical modeling.

106 As an outcome, we identified two major points to be taken into consideration in the formulation
107 of polymer-based medical devices: first, the importance of establishing the impact of the selected
108 terminal sterilization methodology on the polymeric material itself; second, the characterization of
109 the base polymer cannot simply focus on the molecular weight and chemical composition but needs
110 to be extended to other physical parameters. These statements can be used as guidelines for the
111 usage of biodegradable polymers in the production of bioresorbable medical devices.
112

113 2. Materials and Methods

114 2.1. Materials

115 The following chemicals have been used as supplied, without further treatment:
116 poly(L-lactide-co- ϵ -caprolactone) purchased as PLC 70 from Purac-Corbion (The Netherlands),
117 named from now on polymer P; poly(L-lactide-co- ϵ -caprolactone) purchased as RESOMER® LC 703
118 S from Evonik (Germany), named from now on polymer E; tetrahydrofuran (THF) and
119 deuteriochloroform (CDCl₃) purchased from Sigma Aldrich (Germany).

120 2.2. Terminal sterilization procedures

121 Sterilization of a product is properly intended to remove all the living microorganisms
122 contained in or adhering to it, including their resistant dormant bodies, such as *e.g.* spores[23]. When
123 dealing with medical devices this passage is often referred as terminal, because it occurs on the fully
124 finished product, already packed and ready to be sold. A major consequence of this, is the
125 impossibility of analytically testing again each individual device as it would mean removing the
126 packaging and indirectly invalidate the previous sterilization, making all the previous operations
127 useless. Therefore, it is necessary to imply a consolidated, reliable and validated protocol, based on
128 routinely monitored procedures and equipment, which must ensure full sterilization and limited
129 damage on the product. Thus, the selected sterilization conditions must take into consideration, on
130 one hand the number and resistance of microorganisms in the environment in which the treatment is
131 performed and on the other hand the necessity of limited interference with the initial desired
132 characteristics of the final product. All sterilization protocols involved in this work have been
133 conducted in accordance to the aforementioned requirements and are the actual ones currently in
134 use for conventional protocols in the production of biodegradable polymer-based medical devices.

135 2.2.1. Ethylene oxide processing

136 Sterilization via EtO has been performed on both P and E polymers, following a validated
137 protocol, in accordance with the guidelines described in detail in ISO 11135. These procedures take
138 into consideration manufacturing conditions, construction materials and product design, including
139 geometric variability and packaging characteristics (*i.e.* the container must have good EtO
140 permeability).

141 The physical performance qualification allows the verification of the cycle reproducibility as
142 well as the evaluation of the cycle impact on the product, packaging functionality and safety.

143 Specifically, the samples, packed into a sealed, sterile plastic bag and aligned in a rack within a
144 carton box are firstly pre-conditioned for a time range of 105 – 170 min at temperature in range 48 –
145 52°C. Afterwards the cycle starts, first reaching vacuum within a time range of 60 – 120 min at
146 temperature in range 48 – 52°C, and second exposing the product to EtO in gas form for a time of 345
147 – 375 min always at the previous temperature and humidity higher than 60%. The concentration of
148 the gas in this phase is range 320 – 322 g/mc. This last passage is performed at least three times.
149 Finally, a degassing step of 1425 – 1455 min at temperature of 41 – 51°C is performed.

150 2.2.2. Electron beam processing

151 Electron beam sterilization has been applied following a procedure approved and described in
152 the standard ISO 11137. Samples, sealed in glass vials, closed with plastic stopper and aluminum cap
153 and housed in a carton box, were passed through the chamber for few minutes at 47.4 C and
154 invested by a radiation dose in range 25 – 30 kGy. As the beam hits the samples, electrons penetrate
155 the cardboard box and all the samples in their individual packages inside the carton[23]. This
156 ensures that harmful microorganisms are completely inactivated. More specifically, as the electrons
157 penetrate the products, the radiation dose diminishes, therefore, in reality, less radiation leaves the
158 box then entered. Thus, the whole containing boxes are usually turned over and irradiated again
159 from the opposite side in order to get a relatively uniform dose.

160 2.3. Analytical methods

161 Polymer samples have been characterized both before and after each sterilization procedures
162 using the analytical techniques presented in hereby following.

163 2.3.1. Gel permeation chromatography

164 Weight-average (Mw) and number-average molecular weight (Mn) values and molecular
165 weight distributions (Mw/Mn) values of the polymers were evaluated using a Jasco LC-2000Plus
166 gel permeation chromatograph (GPC) equipped with a refractive index detector (RI-2031Plus,
167 Jasco) using 3 Agilent PLgel columns, 5×10^{-6} M particle size, 300×7.5 mm (MW range: 5×10^2 to 17
168 $\times 10^5$ g mol⁻¹). THF was chosen as eluent at a flow rate of 0.5 mL min⁻¹ at 35 °C. The GPC samples
169 were injected using a Jasco AS-2055Plus autosampler. The instrument was calibrated using
170 polystyrene standards from 580 to 3250000 Da (Polymer Laboratories).

171 2.3.2. Differential scanning calorimetry

172 Differential scanning calorimetry (DSC) measurements were conducted using Q1000
173 Differential Scanning Calorimeter (TA Instruments) using 40 µL crucibles in aluminum and a
174 heating and cooling rate of 5°C/min in a nitrogen atmosphere (T ranges: 0 – 200 °C and 0 – 300 °C).

175 2.3.3. X-ray diffraction

176 The crystal structure was investigated by the grazing incident X-ray diffraction (XRD)
177 technique with Cu K-α radiation in Bragg-Brentano configuration with the scanning angle of 3°.

178 2.3.4. Nuclear magnetic resonance (¹H-NMR)

179 Nuclear Magnetic Resonance (¹H-NMR) was run on samples prepared by dissolving 50 mg of
180 species of interest in 3 mL in CDCl₃ and analyzed with H-NMR 300 MHz from Bruker.

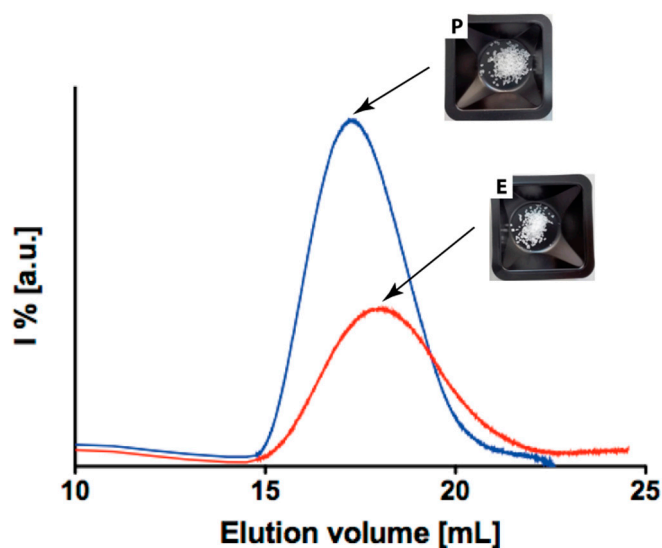
181
182
183
184
185
186

187 3. Results and discussion

188 3.1. Pristine polymer characterization

189 In this section, the characterization of the two pristine polymers is reported. In Figure 1 the GPC
190 chromatograms for both polymer P and E are visible and the characterization results, including also
191 the other analytical techniques, are presented in Table 1. As evident, their initial molecular weight is
192 relatively high in both cases, and the NMR spectra (in S.I.) shows full consistency in their
193 composition, which is confirmed equal to the one declared by suppliers of 70% PLA and 30% PCL
194 (full data in Table 1).

195 On the other hand, still NMR, DSC (Figure 2) data and XRD enable to identify considerable
196 differences between the two polymers (data in Table 1). As a matter of fact, E polymer has a
197 crystallinity degree of 65% whereas P is around 35%. This statement is well supported by the NMR
198 and DSC curve of Figure 2. Indeed, polymer E presents a well for the crystallization temperature, at
199 106°C, and a defined melting point at 160°C, whereas polymer P does not show any of the
200 aforementioned detectable points and the shape of the curve clearly resemble the one of amorphous
201 polymers. Similar conclusion can be drawn when looking at the XRD measurement (in S.I.) that also
202 confirms the partial crystalline nature of E and the amorphous one of P. Indeed, from Scherrer
203 equation we calculated full width at half maximum (FWHM) and average grain size (L_{hkl}) [33] and
204 the more crystalline nature of E sample is evident. Therefore, though the two polymers might look
205 similar from the composition and up to certain extent also from the molecular weight perspective, it
206 is however reasonable to expect different physical behavior and response to the sterilization
207 protocols in dependence on their crystallinity.



208

209 **Figure 1.** GPC chromatograms of P (blue line) and E (red line). Picture of the two pristine polymers as
210 removed from the supplier's packaging.

211

212

213

214

215

216

217

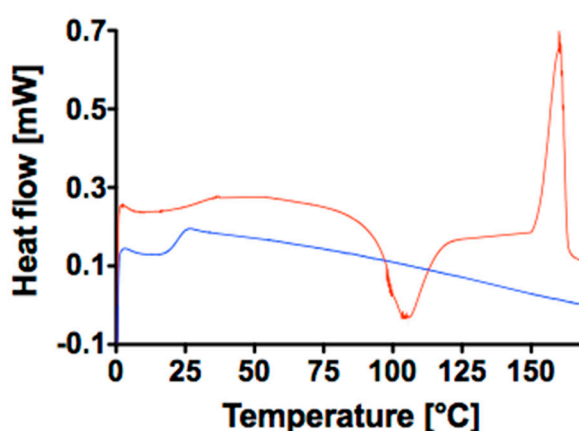
218

219

Table 1. Data obtained by GPC, ¹H-NMR, DSC and XRD of the polymeric samples.

# Sample	GPC			¹ H-NMR		DSC	XRD	
	M _w [Da]	M _n [Da]	PD [-]	CL [%] g/g _{tot}	cristallin ity [%]	cristallin ity [%]	FWHM [°]	L _{hkl} [Å]
E	119600	85660	1.12	25.4	61.1	65	4.5	0.308
P	172750	123800	1.6	25.5	36.1	35.2	7.5	0.185
E EtO	96000	78700	1.2	25	59.6	60	4.5	0.308
P EtO	159400	97300	1.64	25.7	34.3	35	7.5	0.185
E e-beam	51800	43660	1.3	25.6	60.6	59.2	4.5	0.317
P e-beam	133300	64100	2.08	25.4	35.5	32.1	7.5	0.185

220



221

222

Figure 2. DSC curve of P (blue line) and E (red line).

223

3.2. Ethylene oxide processing

224

225

226

227

228

229

230

231

232

233

234

235

236

237

238

239

240

241

Though relatively expensive, ethylene oxide (EtO) processing is widely used for the sterilization of medical devices and surgical instruments and it basically consists in a controlled exposure of the products to ethylene oxide in gaseous form, in a sealed chamber. The high diffusivity of EtO, coupled with its high reactivity, is of major importance for the inactivation of microorganisms. In fact, EtO can penetrate selected packaging and access all the exposed surfaces of the product. Moreover, it works as an alkylating agent for protein essential for cell reproduction, DNA and RNA. This way, it prevents normal cellular metabolism and the ability to reproduce of the affected microbes, which becomes nonviable[24]. In general, the chemical species targeted by EtO are not included in most of the medical devices composition, therefore, their exposure to EtO should have very little or no impact on them, independently on their physical characteristics. On the other hand, the whole process is performed at mid-high temperature and relatively high humidity, both parameters that might affect the polymer initial fashions. Indeed, though not great changes are recorded in the physical characteristics of the polymers (DSC in Figure 3 and XRD in S.I.), still a statistically relevant albeit small reduction of the molecular weights is recorded for both of them (Table 1). As a matter of fact, the M_w of polymer E moves from 119609 Da to 96000 Da, with a change in PD of 0.013, whereas the one of polymer P shifts from 172746 Da to 159413 Da with a PD variation of 0.04 (Figure 4). Though these changes might not be an effect of the EtO directly, it is anyhow rather important to record the inevitable degradation effect given by the whole sterilization protocol.

242

243 3.3. Electron beam processing

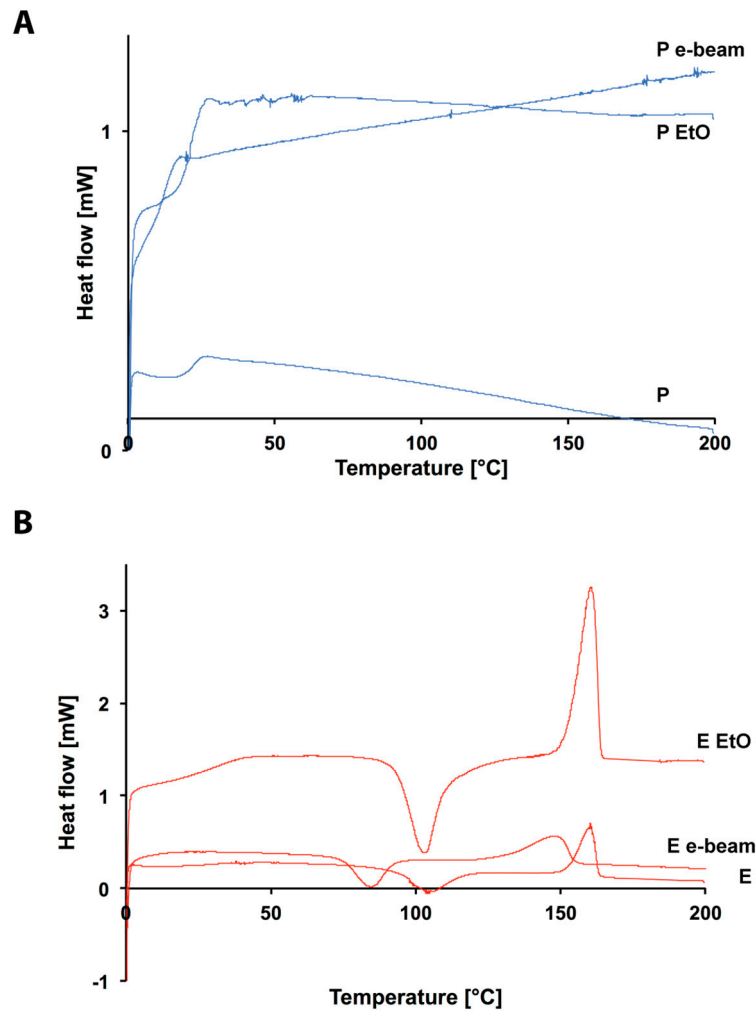
244 Electron beam irradiation processing (e-beam) is commonly used in the sterilization of medical
245 devices and in general represent a much faster and cheaper solution in respect to EtO processing.
246 The procedure involves irradiation of the products with a high-energy electron beam which ionize in
247 a controlled way the hit samples. The bombardment results in a cascade of free electrons through the
248 material domain, which, when interact with surrounding molecules, generate free radicals. These
249 last species induce breaks in the DNA double helix, preventing replication and expression, therefore
250 enabling sterilization effects[23]. Due to its mechanism of action, it is important to limit the duration
251 of the whole irradiation to the minimum (generally just few minutes), otherwise great damage on
252 the final products, such as polymers embrittlement, oxidative damage and color change might
253 occur[34,35]. Indeed, especially for polymer based devices, ionizing radiations exhibit an important
254 side effect that affects their performances, such as decrease in both number and weight average
255 molecular weight and modification of the chains distribution and conformation.

256 Such effect is evident already at the minimal radiation dose (the "overkill dose") that ensures
257 sterilization, equal to 25 kGy[36]. Indeed, the free radicals and ions can also lead to recombination
258 reactions, hydrogen abstraction or cross-linking reactions[37]. Moreover, if radiation energy is
259 higher than intramolecular forces, unzipping reactions (*i.e.* depolymerization reactions) can occur.
260 Generally speaking, the molecular weight decrease is proportional to the radiation dose[37–39].
261 Moreover, the specific trend depends on material composition (which determines the reactions
262 pathways), degree of crystallinity, and sterilization environment (*i.e.* temperature and the presence
263 of air, since oxygen molecules enhance the molecular weight decrease). This phenomenon has an
264 important impact on the final behavior of devices made of aliphatic polyesters which in general
265 reflects on the mechanical properties of the finite device. Indeed, though the Young modulus
266 decreases very slightly, the elongation at break diminishes dramatically, following a
267 dose-dependent trend. In addition, radiations also influence the glass transition temperature,
268 melting temperature and the degree of crystallinity[38,40–42].

269 In general, the two main reactions that take place during irradiation are chain scission and
270 cross-linking[26,28,38,43]. The ratio between methylene and ester groups CH_2/COO is a very
271 important parameter, because it discriminates the structure of the material after irradiation dose[38].
272 In particular, for high values of CH_2/COO ratio cross-linking is the dominant kinetic mechanism,
273 while at low values polymer degradation mainly occurs.

274 In particular, polyglycolic acid exhibits the lowest CH_2/COO ratio and experiences degradation
275 while irradiated; cross-linking reactions appear only after very high radiation doses. Regarding the
276 considered example of poly(L-lactide-co- ϵ -caprolactone), as one can see from Table 1, a clear
277 decrease after irradiation in molecular weight M_w for both polymers E and P is observable. Indeed,
278 the final values are 51814 Da for E and 133265 Da for P. In this sense, this is a huge difference in
279 respect to the previously discussed EtO sterilization treatment. Moreover, though the variation of
280 polymer P might appear to be smaller than the case of E, this result has to be taken into consideration
281 in light also of the PD values of both distributions. As evident from Table 1 it varies considerably
282 between the two polymers: E shows a variation of 0.113 whereas P one of 0.48. This means, that in
283 the case of P much more oligomers are produced upon irradiation so that the distribution
284 considerably enlarges. Therefore, clearly it would be more difficult, from a process perspective, to
285 rely on the selected initial properties of the pristine material. On the other hand, polymer E almost
286 preserves its intrinsic polydispersity making the effect of the treatment on the final properties of the
287 finished device more easily predictable. The difference that is observed within the two ionized
288 polymers can be explained by the mechanism of action of the radical species. Indeed, if they find
289 themselves confined in close proximity within the highly-ordered arrangement of chains ("cage") in
290 the crystalline domain it is easier for them to recombine rather than diffuse out and propagate,
291 reducing the effective chain scissions and making it occur in a rather more controlled way within the
292 crystalline domain. On the other hand, such a "cage effect" is certainly less expected for amorphous
293 arrangements, where much more free space is left to the radicals to diffuse and propagate randomly
294 through the overall polymer network[28,43].

295 Moreover, though the actual composition is left untouched (NMR in S.I.) detectable
296 modifications are recorded also in the crystallinity of the two polymers upon irradiation. Indeed, the
297 crystallinity degree of E is reduced and the actual well for the point of crystallization is shifted from
298 100°C for the pristine polymer to 87°C for the ionized one. Such changes are not easy to detect for the
299 case of P, as already in its pristine appearance, it presents an amorphous nature, whose DSC curve
300 does not present any noticeable wells or peaks (Figure 3).
301



302
303
304

Figure 3. DSC curves of: A) P, P EtO and P e-beam (blue lines); B) E, E EtO and E e-beam (blue lines).

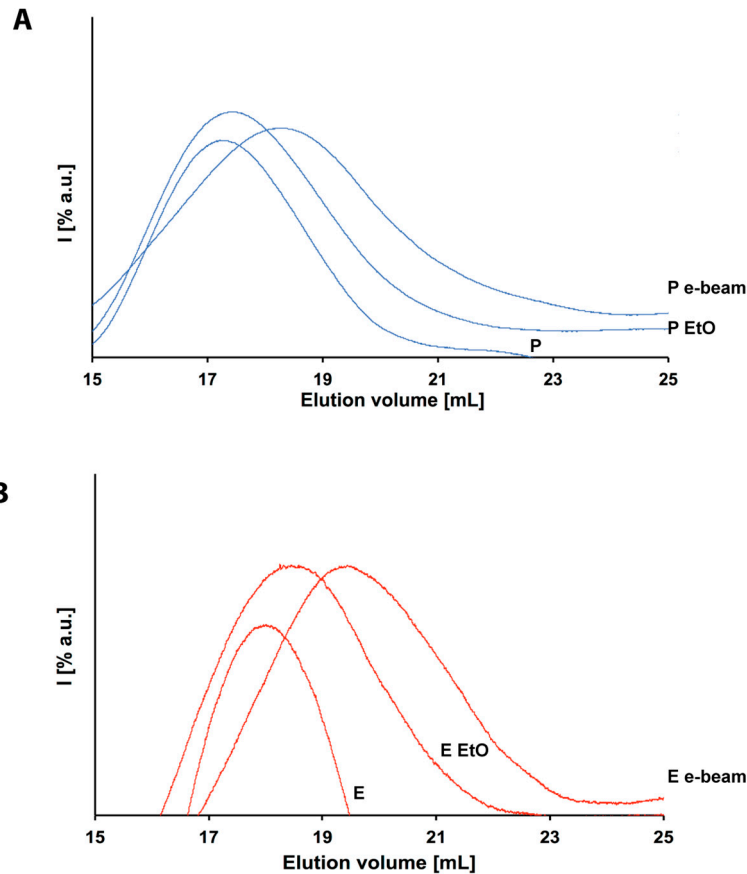


Figure 4. GPC chromatograms of: A) P, P EtO and P e-beam (blue lines); B) E, E EtO and E e-beam (blue lines).

305
306
307
308

309 3.4. Mathematical modelling

310 Electron beam sterilization not only alters the initial polymer properties, but also accelerates the
311 degradation rate. This cannot be disregarded, because a faster decay of the molecular weight reduces
312 the time span where, *e.g.*, a device can assure the desired mechanical properties. Therefore, a
313 comprehensive overview of the consequences of electron beam sterilization should couple the
314 analysis of the detrimental effects on raw material as well as its accelerated degradation.

315 For this purpose, mathematical modeling emerges as a useful tool that can provide a
316 quantitative estimation of the molecular weight decay. In this framework, the model proposed by
317 Perale *et al.*[44] and Casalini *et al.*[45] has been chosen for the comprehensive description of the
318 involved phenomena (hydrolysis, autocatalysis and transport phenomena) and its validated results.
319 Details are extensively discussed in previous papers[44,45], but model formulation is here
320 summarized for the sake of completeness.

321 The model is based on population balances, where a mass balance for a polymer chain with n
322 repeating units is written. Since it is necessary to write an equation for each considered chain length
323 value, this approach would imply a large number of differential equation to be solved (about 10^5). In
324 order to reduce the computational effort, the method of the statistical moment is employed[46],
325 allowing to reduce the large number of population balance equations to three equations, which
326 accounts for the time and spatial evolution of the statistical moments of the first three orders.

327
328
329
330

331 The generic j-th order moment μ_j is defined as follows:

$$332 \mu_j = \sum_{n=1}^{\infty} n^j C_n \quad (1)$$

333 where n is chain length and C_n is the concentration of a polymer chain with n repeating units.

334 Under the assumption that only oligomers up to nonamers can diffuse through polymer matrix,
335 model is composed by a system of partial differential equations that account for time and spatial
336 evolution of monomer (eq. 2), water (eq. 3), oligomers (eq. 4) and statistical moments of zero-th, first
337 and second order (eqs. 5 – 7):

$$338 \frac{\partial C_M}{\partial t} = \nabla(D_M \nabla C_M) + 2k_d C_W (\mu_0 - C_M) \mu_0 \quad (2)$$

$$339 \frac{\partial C_W}{\partial t} = \nabla(D_W \nabla C_W) - k_d C_W (\mu_1 - \mu_0) \mu_0 \quad (3)$$

$$340 \frac{\partial C_n}{\partial t} = \nabla(D_{olig} \nabla C_n) + 2k_d C_W (\mu_0 - \sum_{j=1}^n C_j) \mu_0 - (n-1)k_d C_W C_n \mu_0 \quad 2 \leq n \leq 9 \quad (4)$$

$$341 \frac{\partial \mu_0}{\partial t} = \sum_{j=1}^9 \nabla(D_j \nabla C_j) + k_d C_W (\mu_1 - \mu_0) \mu_0 \quad (5)$$

$$342 \frac{\partial \mu_1}{\partial t} = \sum_{j=1}^9 j \cdot \nabla(D_j \nabla C_j) \quad (6)$$

$$343 \frac{\partial \mu_2}{\partial t} = \sum_{j=1}^9 j^2 \cdot \nabla(D_j \nabla C_j) + \frac{k_d C_W \mu_0}{3} \left(\mu_1 - 2 \frac{\mu_2}{\mu_1} + \frac{\mu_2 \mu_1}{\mu_0} \right) \quad (7)$$

344 Where C_M is monomer concentration, D_M is monomer diffusion coefficient, k_d is degradation
345 kinetic constant, C_W is water concentration, D_W is water diffusion coefficient, C_n is the concentration
346 of an oligomer with n repeating units and D_{olig} is oligomer diffusion coefficient.

347 The model takes into account the increase of diffusivity due to degradation (chain scissions
348 open new and wider diffusive path) through the following expression:

$$349 D_i = D_i^0 \exp \left[2.5 \left(1 - \frac{M_n(t,x)}{M_n(t=0)} \right)^{0.5} \right] \quad i = \text{monomer, oligomer, water} \quad (8)$$

350 Where D_i^0 is the diffusion coefficient of the i-th species before degradation onset, and x is a
351 generic spatial coordinate.

352 The average properties of interest, such as number average molecular weight M_n , weight
353 average molecular weight M_w and polydispersity PD can be easily calculated starting from the
354 statistical moments:

$$355 M_n = \frac{\mu_1}{\mu_0} M_{mon} \quad (9)$$

$$356 M_w = \frac{\mu_2}{\mu_1} M_{mon} \quad (10)$$

$$357 PD = \frac{\mu_2 \mu_0}{\mu_1^2} \quad (11)$$

358 where M_{mon} is the molecular weight of the repeating unit.

359 Model equations are here written in their general form, but only one spatial coordinate (the
360 characteristic diffusion length) is usually considered in the Laplacian term. The system of partial
361 differential equations constituted by eqs. 2 – 7 is solved through the method of lines: spatial
362 derivatives are approximated through a finite difference scheme (centered formulation) and the
363 resulting system of ordinary differential equations is numerically integrated by means of *ode15s*
364 algorithm implemented in MATLAB.

365 The analysis has been performed starting from experimental data taken from Loo *et al.*[26],
366 chosen as a reference case for their exhaustiveness; in particular, Loo and coworkers studied the
367 influence of irradiation dose on the initial properties and hydrolytic degradation of electron beam –
368 irradiated films of polylactic acid.

369

379 The mathematical model has been used in order to compute a degradation kinetic constant,
 380 which offers a quantitative estimation of the degradation enhancement provided by electron beam
 381 sterilization; film thickness has been considered as characteristic diffusion length. Kinetic constants
 382 have been obtained through fitting of experimental data, in order to best reproduce the decay of the
 383 number average molecular weight over time; data fitting has been carried out by means of *lsqnonlin*
 384 algorithm implemented in MATLAB. Model input parameters are summarized in Table 2.

385
 386

Table 2. Model input parameters

Film thickness [μm]	55
Mmon [g mol^{-1}]	90.08
q_{pol}	1.2
D_M⁰ [$\text{cm}^2 \text{s}^{-1}$]	10^{-10}
D_{olig}⁰ [$\text{cm}^2 \text{s}^{-1}$]	10^{-10}
D_w⁰ [$\text{cm}^2 \text{s}^{-1}$]	10^{-8}

387

388 Initial conditions and kinetic constants are summarized in Table 3, while a comparison between
 389 model results and experimental data is shown in Figure 5A.

390

391 **Table 3.** Initial properties of the polymer analyzed through mathematical modeling and degradation
 392 kinetic constants obtained through experimental data fitting.

Radiation dose [Mrad]	Number average molecular weight [g mol^{-1}]	Polydispersity [-]	Degradation constant [$\text{cm}^6 \text{mol}^{-2} \text{s}^{-1}$]
0	406000	1.60	$3.85 \cdot 10^{-5}$
5	64700	1.68	$1.27 \cdot 10^{-4}$
10	43200	1.73	$1.47 \cdot 10^{-4}$
20	23100	1.76	$1.21 \cdot 10^{-4}$

393

394

395

396

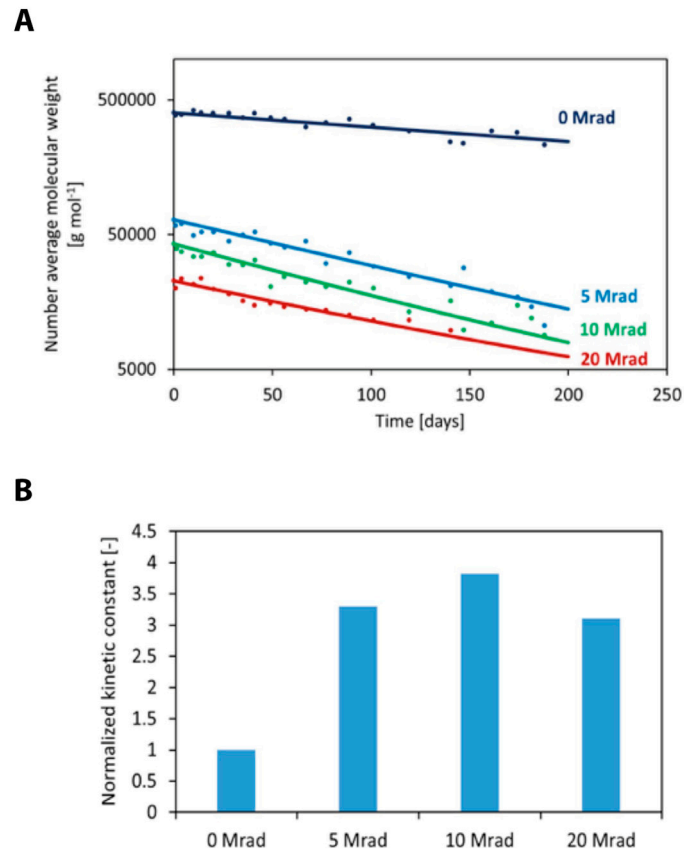


Figure 5. Comparison between model predictions (continuous line) and experimental data (filled circles) taken from Loo et al.[26] for different radiation doses (a). Normalized degradation kinetic constants as a function of radiation dose. Values have been normalized with respect to the kinetic constant of the non-irradiated polymer (b).

Model best fitting is in good agreement with experimental data, thus confirming the reliability of the chosen approach. The obtained kinetic constants are listed in Table 3, while the normalized values are shown in Figure 5B. In particular, values have been normalized choosing the non-irradiated polymer as reference value. *In primis*, data confirm that electron beam sterilization accelerates polymer degradation, since it reduces the initial molecular weight through chain scission. According to model results, hydrolysis is about 3.5 times faster for the irradiated polymer; in addition, degradation enhancement does not depend on radiation dose, since the values of the kinetic constants are close to each other.

This analysis highlights that, for an optimal device design, the initial molecular weight drop due to irradiation must be coupled with the enhanced degradation in order to identify the most suitable polymer. In other words, the choice of the raw material (*i.e.*, before sterilization and processing) should take into account that the initial molecular weight will be not only reduced by processing and sterilization but will also decay faster. This is essential for those applications where the device must assure, *e.g.*, mechanical stability in a determined time span.

397
398
399
400
401
402
403
404
405
406
407
408
409
410
411
412
413
414
415
416
417
418
419
420
421
422
423
424

425 **4. Conclusions**

426 In this work we presented a case study for showing a possible methodologic approach for the
427 selection of appropriate biodegradable polymers in product formulation for medical devices
428 manufacturing. In particular, the major effect of the finished product terminal sterilization is
429 discussed and a comparison between the EtO and e-beam treatments is presented for two apparently
430 similar poly(L-lactide-co- ϵ -caprolactone) base materials with identical composition (70% PLA and
431 30% PCL). Specifically, the major difference resembles in the degree of crystallinity of the
432 aforementioned polymer: E has a relatively high degree of 65% whereas P a rather amorphous
433 structure. Once sterilized, independently on the implied sterilization protocol, both polymers
434 exhibited degradation. Actually, the EtO exposition minimally affected the initial characteristics (in
435 terms of M_w , PD and crystallinity), whereas major differences before and after the treatment was
436 observed for e-beam irradiation. Indeed, a major reduction in molecular weight was observed for
437 both polymers. Additionally, the different chains arrangement led to different response to the
438 treatment. Indeed, even if polymer P degraded apparently less than polymer E, the chain length
439 distribution considerably broadened. This would reflect in a more uncontrolled change in the
440 desired initial properties selected during product formulation and design. Moreover, irradiation has
441 also a major effect on the degradation kinetic of polymers. This effect has been studied through a
442 mathematical model, which allowed to identify that hydrolysis is about 3.5 times faster for the
443 irradiated polymer than to pristine one, remarkably not being dependent on the radiation dose.

444 As a conclusion, we believe that the presented example might be very useful in the
445 development of bioresorbable devices. As a matter of fact, intrinsic response of the material upon the
446 overall post-processing steps might be understood only upon a deep and appropriate
447 characterization of the starting polymers, even when they are nominally similar.

448
449
450
451

452 **Supplementary Materials:** The following are available online, Figure S1: NMR spectra of P and E samples,
453 Figure S2: XRD spectra of P (blue line) and E (red line), Figure S3: NMR spectra of P and E after EtO, Figure S4:
454 XRD spectra of P (blue line) and E (red line) after EtO, Figure S5: NMR spectra of P and E after electron beam
455 irradiation, Figure S6: XRD spectra of P and E after electron beam irradiation.

456 **Author Contributions:** Conceptualization, A.C., F.R. and G.P.; Experiments, A.C., S.C., A.K. M.S. and F. R.;
457 Mathematical modeling T.C.; Writing-Original Draft Preparation, A.C. and T.C.; Writing-Review & Editing, ,
458 A.C., T.C., A.C., A.K., M.S., F.R. and G.P.; Supervision A.C., T.C., F.R. and G.P.

459 **Funding:** This research received no external funding.

460 **Conflicts of Interest:** The authors declare no conflict of interest.

461

462 **References**

- 463 1. Perale, G.; Hilborn, J. *Bioresorbable Polymers for Biomedical Applications - From Fundamentals to*
464 *Translational Medicine*; 1st ed.; Woodhead Publishing Series in Biomaterials, 2016;
- 465 2. Cameron, R. E.; Kamvari-Moghaddam, A. *Synthetic bioresorbable polymers*; Woodhead
466 Publishing Limited, 2012; ISBN 9781845699291.
- 467 3. Planell, J. A. *Bone Repair Biomaterials*; Woodhead Publishing Limited, 2009; ISBN
468 9781845693763.
- 469 4. Armentano, I.; Bitinis, N.; Fortunati, E.; Mattioli, S.; Rescignano, N.; Verdejo, R.;
470 Lopez-Manchado, M. A.; Kenny, J. M. Multifunctional nanostructured PLA materials for
471 packaging and tissue engineering. *Prog. Polym. Sci.* **2013**, *38*, 1720–1747,
472 doi:10.1016/j.progpolymsci.2013.05.010.
- 473 5. Ceccarelli, G.; Presta, R.; Benedetti, L.; Cusella De Angelis, M. G.; Lupi, S. M.; Rodriguez Y
474 Baena, R. Emerging Perspectives in Scaffold for Tissue Engineering in Oral Surgery. *Stem*
475 *Cells Int.* **2017**, *2017*, doi:10.1155/2017/4585401.
- 476 6. Athanasiou, K. A.; Niederauer, G. G.; Agrawal, C. M. Sterilization, toxicity, biocompatibility
477 and clinical applications of polylactic acid/polyglycolic acid copolymers. *Biomaterials* **1996**, *17*,
478 93–102, doi:10.1016/0142-9612(96)85754-1.
- 479 7. Casalini, T.; Perale, G. Types of bioresorbable polymers for medical applications. *Durab.*
480 *Reliab. Med. Polym.* **2012**, 3–29, doi:10.1016/B978-1-84569-929-1.50001-5.
- 481 8. Farah, S.; Anderson, D. G.; Langer, R. Physical and mechanical properties of PLA, and their
482 functions in widespread applications — A comprehensive review. *Adv. Drug Deliv. Rev.* **2016**,
483 *107*, 367–392, doi:10.1016/j.addr.2016.06.012.
- 484 9. Sheikh, Z.; Najeeb, S.; Khurshid, Z.; Verma, V.; Rashid, H.; Glogauer, M. Biodegradable
485 materials for bone repair and tissue engineering applications. *Materials (Basel)*. **2015**, *8*, 5744–
486 5794, doi:10.3390/ma8095273.
- 487 10. Miller, N. D.; Williams, D. F. The in vivo and in vitro degradation of poly(glycolic acid)
488 suture material as a function of applied strain. *Biomaterials* **1984**, *5*, 365–368,
489 doi:10.1016/0142-9612(84)90037-1.
- 490 11. Prakasam, M.; Locs, J.; Salma-Ancane, K.; Loca, D.; Largeteau, A.; Berzina-Cimdina, L.
491 Biodegradable Materials and Metallic Implants—A Review. *J. Funct. Biomater.* **2017**, *8*, 44,
492 doi:10.3390/jfb8040044.
- 493 12. Santoro, M.; Perale, G. Using synthetic bioresorbable polymers for orthopedic tissue
494 regeneration. *Durab. Reliab. Med. Polym.* **2012**, 119–139,
495 doi:10.1016/B978-1-84569-929-1.50006-4.
- 496 13. Colombo, C.; Gatti, S.; Ferrari, R.; Casalini, T.; Cuccato, D.; Morosi, L.; Zucchetti, M.;
497 Moscatelli, D. Self-assembling amphiphilic PEGylated block copolymers obtained through
498 RAFT polymerization for drug-delivery applications. *J. Appl. Polym. Sci.* **2016**, *133*, 1–8,
499 doi:10.1002/app.43084.

- 500 14. Kumari, A.; Yadav, S. K.; Yadav, S. C. Biodegradable polymeric nanoparticles based drug
501 delivery systems. *Colloids Surfaces B Biointerfaces* **2010**, *75*, 1–18,
502 doi:10.1016/j.colsurfb.2009.09.001.
- 503 15. Ferrari, R.; Cingolani, A.; Moscatelli, D. Solvent effect in PLA-PEG based nanoparticles
504 synthesis through surfactant free polymerization. *Macromol. Symp.* **2013**, *324*,
505 doi:10.1002/masy.201200073.
- 506 16. Ferrari, R.; Yu, Y.; Morbidelli, M.; Hutchinson, R. A.; Moscatelli, D. ϵ -Caprolactone-Based
507 Macromonomers Suitable for Biodegradable Nanoparticles Synthesis Through Free Radical
508 Polymerization. *Macromolecules* **2011**, *44*, 9205–9212, doi:10.1021/ma201955p.
- 509 17. Pillai, C. K. S.; Sharma, C. P. Review paper: Absorbable polymeric surgical sutures:
510 Chemistry, production, properties, biodegradability, and performance. *J. Biomater. Appl.* **2010**,
511 *25*, 291–366, doi:10.1177/0885328210384890.
- 512 18. Peppas, N. A.; Bures, P.; Leobandung, W.; Ichikawa, H. Hydrogels in pharmaceutical
513 formulations. *Eur. J. Pharm. Biopharm.* **2000**, *50*, 27–46, doi:10.1016/S0939-6411(00)00090-4.
- 514 19. Freed, L. E.; Vunjak-Novakovic, G.; Biron, R. J.; Eagles, D. B.; Lesnoy, D. C.; Barlow, S. K.;
515 Langer, R. Biodegradable Polymer Scaffolds for Tissue Engineering. *Nat. Biotechnol.* **1994**, *12*,
516 1119–1124, doi:10.1038/ng1294-340.
- 517 20. Kutz, M. *Applied Plastics Engineering Handbook*; Elsevier Inc., 2011;
- 518 21. Lambert, B. J.; Mendelson, T. A.; Craven, M. D. Radiation and Ethylene Oxide Terminal
519 Sterilization Experiences with Drug Eluting Stent Products. *AAPS PharmSciTech* **2011**, *12*,
520 1116–1126, doi:10.1208/s12249-011-9644-8.
- 521 22. Dearth, C. L.; Keane, T. J.; Carruthers, C. A.; Reing, J. E.; Huleihel, L.; Ranallo, C. A.; Kollar, E.
522 W.; Badylak, S. F. The effect of terminal sterilization on the material properties and in vivo
523 remodeling of a porcine dermal biologic scaffold. *Acta Biomater.* **2016**, *33*, 78–87,
524 doi:10.1016/j.actbio.2016.01.038.
- 525 23. Tipnis, N. P.; Burgess, D. J. Sterilization of implantable polymer-based medical devices: A
526 review. *Int. J. Pharm.* **2018**, *544*, 455–460, doi:10.1016/j.ijpharm.2017.12.003.
- 527 24. C Mendes, G. C.; S Brandão, T. R.; M Silva, C. L. Ethylene oxide sterilization of medical
528 devices: A review. *Am J Infect Control* **2007**, *35*, 574–581, doi:10.1016/j.ajic.2006.10.014.
- 529 25. McKeen, L. *Effect of Sterilization Method on Plastics and Elastomers*; 3rd ed.; Elsevier Inc., 2012;
- 530 26. Loo, S. C. J.; Tan, H. T.; Ooi, C. P.; Boey, Y. C. F. Hydrolytic degradation of electron beam
531 irradiated high molecular weight and non-irradiated moderate molecular weight PLLA. *Acta*
532 *Biomater.* **2006**, *2*, 287–296, doi:10.1016/j.actbio.2005.10.003.
- 533 27. Loo, S. C. J.; Ooi, C. P.; Boey, Y. C. F. Radiation effects on poly(lactide-co-glycolide) (PLGA)
534 and poly(L-lactide) (PLLA). *Polym. Degrad. Stab.* **2004**, *83*, 259–265,
535 doi:10.1016/S0141-3910(03)00271-4.

536

537

- 538 28. Loo, J. S. C.; Ooi, C. P.; Boey, F. Y. C. Degradation of poly(lactide-co-glycolide) (PLGA) and
539 poly(L-lactide) (PLLA) by electron beam radiation. *Biomaterials* **2005**, *26*, 1359–1367,
540 doi:10.1016/j.biomaterials.2004.05.001.
- 541 29. Pertici, G. The effect of molecular structure on the properties of biomedical polymers. *Durab.*
542 *Reliab. Med. Polym.* **2012**, 30–48, doi:10.1016/B978-1-84569-929-1.50002-7.
- 543 30. Roato, I.; Belisario, D. C.; Compagno, M.; Verderio, L.; Sighinolfi, A.; Mussano, F.; Genova, T.;
544 Veneziano, F.; Pertici, G.; Perale, G.; Ferracini, R. Adipose-Derived Stromal Vascular
545 Fraction/Xenohybrid Bone Scaffold: An Alternative Source for Bone Regeneration. *Stem Cells*
546 *Int.* **2018**, *2018*, 1–11, doi:10.1155/2018/4126379.
- 547 31. D’Alessandro, D.; Perale, G.; Milazzo, M.; Moscato, S.; Stefanini, C.; Pertici, G.; Danti, S.
548 Bovine bone matrix/poly(L-lactic-co- ϵ -caprolactone)/gelatin hybrid scaffold (SmartBone®)
549 for maxillary sinus augmentation: A histologic study on bone regeneration. *Int. J. Pharm.*
550 **2017**, *523*, 534–544, doi:10.1016/j.ijpharm.2016.10.036.
- 551 32. Pertici, G.; Carinci, F.; Carusi, G.; Epistatus, D.; Villa, T.; Crivelli, F.; Rossi, F.; Perale, G.
552 Composite Polymer-Coated Mineral Scaffolds for Bone Regeneration: From Material
553 Characterization To Human Studies. *J. Biol. Regul. Homeost. Agents* **2015**, *29*, 136–148.
- 554 33. Scardi, P.; Leoni, M.; Delhez, R. Line broadening analysis using integral breadth methods: A
555 critical review. *J. Appl. Crystallogr.* **2004**, *37*, 381–390, doi:10.1107/S0021889804004583.
- 556 34. Xiao, L.; Wang, B.; Yang, G.; Gauthier, M. Poly (Lactic Acid) -Based Biomaterials : Synthesis ,
557 Modification and Applications. **2006**, doi:10.5772/23927.
- 558 35. Cairns, M. L.; Sykes, A.; Dickson, G. R.; Orr, J. F.; Farrar, D.; Dumba, A.; Buchanan, F. J.
559 Through-thickness control of polymer bioresorption via electron beam irradiation. *Acta*
560 *Biomater.* **2011**, *7*, 548–557, doi:10.1016/j.actbio.2010.09.012.
- 561 36. Nguyen, H.; Morgan, D. A. F.; Forwood, M. R. Sterilization of allograft bone: Is 25 kGy the
562 gold standard for gamma irradiation? *Cell Tissue Bank.* **2007**, *8*, 81–91,
563 doi:10.1007/s10561-006-9019-7.
- 564 37. Guo, C.; Zhou, L.; Lv, J. Effects of expandable graphite and modified ammonium
565 polyphosphate on the flame-retardant and mechanical properties of wood
566 flour-polypropylene composites. *Polym. Polym. Compos.* **2013**, *21*, 449–456, doi:10.1002/app.
- 567 38. Narkis, M.; Sibony-Chaouat, S.; Siegmann, A.; Shkolnik, S.; Bell, J. P. Irradiation effects on
568 polycaprolactone. *Polymer (Guildf).* **1985**, *26*, 50–54, doi:10.1016/0032-3861(85)90056-4.
- 569 39. Gupta, M. C.; Deshmukh, V. G. Radiation effects on poly(lactic acid). *Polymer (Guildf).* **1983**,
570 *24*, 827–830, doi:10.1016/0032-3861(83)90198-2.
- 571 40. Filipczak, K.; Wozniak, M.; Ulanski, P.; Olah, L.; Przybytniak, G.; Olkowski, R. M.;
572 Lewandowska-Szumiel, M.; Rosiak, J. M. Poly(ϵ -caprolactone) biomaterial sterilized by
573 E-beam irradiation. *Macromol. Biosci.* **2006**, *6*, 261–273, doi:10.1002/mabi.200500215.
- 574 41. Gandhi, K.; Kriz, D.; Salovey, R.; Narkis, M.; Wallerstein, R. Crosslinking of polycaprolactone
575 in the pre-gelation region. *Polym. Eng. Sci.* **1988**, *28*, 1484–1490, doi:10.1002/pen.760282209.

- 576 42. Oláh, L.; Filipczak, K.; Czvikovszky, T.; Czigány, T.; Borbás, L. Changes of porous
577 poly(ϵ -caprolactone) bone grafts resulted from e-beam sterilization process. *Radiat. Phys.*
578 *Chem.* **2007**, *76*, 1430–1434, doi:10.1016/j.radphyschem.2007.02.046.
- 579 43. Loo, S. C. J.; Ooi, C. P.; Boey, Y. C. F. Influence of electron-beam radiation on the hydrolytic
580 degradation behaviour of poly(lactide-co-glycolide) (PLGA). *Biomaterials* **2005**, *26*, 3809–3817,
581 doi:10.1016/j.biomaterials.2004.10.014.
- 582 44. Perale, G.; Arosio, P.; Moscatelli, D.; Barri, V.; Müller, M.; Maccagnan, S.; Masi, M. A new
583 model of resorbable device degradation and drug release: Transient 1-dimension diffusional
584 model. *J. Control. Release* **2009**, *136*, 196–205, doi:10.1016/j.jconrel.2009.02.014.
- 585 45. Casalini, T.; Rossi, F.; Lazzari, S.; Perale, G.; Masi, M. Mathematical modeling of PLGA
586 microparticles: From polymer degradation to drug release. *Mol. Pharm.* **2014**, *11*, 4036–4048,
587 doi:10.1021/mp500078u.
- 588 46. Ramkrishna, D. *Population Balances - Theory and Applications to Particulate Systems in*
589 *Engineering*; Elsevier Inc., 2000